Appl. Math. Mech. -Engl. Ed., **44**(8), 1305–1316 (2023)

APPLIED MATHEMATICS AND MECHANICS (ENGLISH EDITION)

https://doi.org/10.1007/s10483-023-3012-5

A symplectic finite element method based on Galerkin discretization for solving linear systems*

Zhiping QIU†, Zhao WANG, Bo ZHU

Institute of Solid Mechanics, School of Aeronautic Science and Engineering,
Beihang University, Beijing 100083, China

(Received Nov. 26, 2022 / Revised May 8, 2023)

Abstract We propose a novel symplectic finite element method to solve the structural dynamic responses of linear elastic systems. For the dynamic responses of continuous medium structures, the traditional numerical algorithm is the dissipative algorithm and cannot maintain long-term energy conservation. Thus, a symplectic finite element method with energy conservation is constructed in this paper. A linear elastic system can be discretized into multiple elements, and a Hamiltonian system of each element can be constructed. The single element is discretized by the Galerkin method, and then the Hamiltonian system is constructed into the Birkhoffian system. Finally, all the elements are combined to obtain the vibration equation of the continuous system and solved by the symplectic difference scheme. Through the numerical experiments of the vibration response of the Bernoulli-Euler beam and composite plate, it is found that the vibration response solution and energy obtained with the algorithm are superior to those of the Runge-Kutta algorithm. The results show that the symplectic finite element method can keep energy conservation for a long time and has higher stability in solving the dynamic responses of linear elastic systems.

Key words Galerkin finite element method, linear system, structural dynamic response, symplectic difference scheme

Chinese Library Classification O327
2010 Mathematics Subject Classification 74H15, 74H45

1 Introduction

For linear or nonlinear elastic systems, in the absence of external force and dissipation, all real physical processes can be represented by the Hamiltonian system, and the total energy of the system is conserved. This important property is of great significance in engineering. When the analytical solution of the physical quantity of the system cannot be obtained, we usually use the numerical calculation method to solve the problem. However, with the increase in time steps, the cumulative error brought by the numerical calculation method will make the

* Citation: QIU, Z. P., WANG, Z., and ZHU, B. A symplectic finite element method based on Galerkin discretization for solving linear systems. *Applied Mathematics and Mechanics* (*English Edition*), **44**(8), 1305–1316 (2023) https://doi.org/10.1007/s10483-023-3012-5

† Corresponding author, E-mail: zpqiu@buaa.edu.cn

Project supported by the National Natural Science Foundation of China (Nos. 12132001 and 52192632)

calculation results beyond recognition, making it a highly challenging problem to be accurately solved[1–7]. Therefore, it is of great research value to construct a non-dissipative numerical method in the Hamiltonian system.

Feng[8] first systematically studied the symplectic geometry algorithm based on the Hamiltonian system. Then, he developed a series of symplectic preserving algorithms[9]. Each step of the symplectic geometry algorithm is a symplectic transformation and pioneering research on this system with different methods is carried out[10]. For symplectic algorithms, the calculation results have long-term stable tracking ability. After that, the symplectic preserving algorithm has attracted more and more attention. The condition that the Runge-Kutta method is symplectic was found in 1988 by Sanz-Serna[11], Lasagni[12], and Suris[13] independently. A multi-symplectic algorithm that maintains the symplectic conservation law under the symplectic method similar to the Hamilton ordinary differential equation was proposed by Bridges and Thomas[14] and Reich[15] around 2000. In order to prevent the occurrence of energy drift, the symplectic method was applied to the discretization of the time domain to construct symplectic finite element[16].

Symplectic algorithm has been widely used in engineering and solving equations. Discontinuous Galerkin (DG) method was introduced into the acoustic equation, two-dimensional Maxwell equation, and hyperbolic equation to realize space discretization[17]. The Hamiltonian structure was obtained by mixing and discretizing the acoustic equation and the symplectic method in the time domain, to prevent the loss of energy[18]. Another finite element method uses the Hamilton discontinuous Galerkin (HDG) scheme to discretize space, and uses symplectic, diagonal implicit, and explicit partitioned Runge-Kutta methods to discretize time, ensuring the conservation of energy[19]. Then, the DG method with arbitrary accuracy was introduced into the elastic wave equation, which can maintain the energy or projectile dissipation performance[20]. Qiu and Jiang[21] introduced a symplectic conservative perturbation series expansion method for linear Hamiltonian systems with perturbations and their applications. Qiu and Xia[22] introduced a symplectic perturbation series methodology for a non-conservative linear Hamiltonian system with damping. There are multi-source uncertainties in practical engineering. Qiu and Jiang[23] introduced random and interval linear uncertainties into the nonlinear homogeneous Hamiltonian equation. Later, Qiu and Jiang[24] used random and interval linear uncertainties in the symplectic preserving algorithm of the Birkhoffian system, and compared the calculation results of the two methods. Zhou et al.[25] analyzed the crack propagation along the bi-material interface using the analytical symbolic dual approach. Su et al.[26] proposed an order-modified symplectic finite element method to deal with large-scale seismic wave problems to improve accuracy. Sun et al.[27] constructed the Hamiltonian canonical equation to transform the buckling analysis of ring-stiffened porous graphene sheet-reinforced composite cylindrical shells under hydrostatic pressure into an eigenproblem in symplectic space. Lai et al.[28] solved the torsional buckling problem of cylindrical shells with local defects by the symplectic method. Chen and Zhu[29] introduced the symplectic algorithm into the control theory. Zhou et al.[30] proposed a new method based on a series of analytical symplectic eigensolutions to solve the steady-state forced vibration of composite nanobeam system on an elastic foundation.

Although the symplectic algorithm has been applied in many fields, there is relatively little research on the symplectic algorithm for computing complex continuum. In practical engineering, the finite element method is usually used to discretize complex structures into elements, but this method cannot maintain symplectic structure when solving structural dynamics. In order to maintain the symplectic structure of the discrete system, the fully discrete system is transformed into a Hamiltonian structure, which is solved by using the difference scheme that maintains the symplectic structure. When the spatial discretization of the system is the finite element method, this method is called Hamiltonian symplectic finite element (HSFE). The main work of this paper is to develop a new symplectic finite element method to solve the vibration response of linear elastic systems. This method can maintain the Hamiltonian energy

conservation and long-term stable tracking ability. The linear elastic body is discretized into finite elements, and the Hamiltonian system of the element is constructed. The Hamiltonian system is transformed into the Birkhoffian system by generalized transformation, and then the symplectic scheme of the Birkhoffian system is obtained. In the end, the whole linear elastic body system is constructed, and the Euler midpoint scheme is used to solve the problem.

The contents of this paper are as follows. In Section 2, the linear Hamiltonian system is briefly introduced. In Section 3, the Birkhoffian system is introduced. In Section 4, the Hamiltonian system is discretized by the Galerkin finite element method, the linear Birkhoffian system is established, and the problem is solved by the Euler midpoint scheme. In Section 5, the numerical examples of the linear Hamiltonian function, the vibration response of the Bernoulli-Euler beam, and the vibration response of composite plate demonstrate that the HSFE method can keep energy conservation in a long term. Compared with the classical Runge-Kutta algorithm, the HSFE method has better accuracy and stability. Finally, some concluding remarks are collected in Section 6.

2 Linear Hamiltonian system

Consider an n-dimensional Hamiltonian system. The Hamilton canonical equation is in a compact form of

$$\dot{\boldsymbol{z}} = \frac{\mathrm{d}\boldsymbol{z}}{\mathrm{d}t} = \boldsymbol{J}^{-1} H_{\boldsymbol{z}}, \tag{1}$$

where

$$\begin{cases} \boldsymbol{z} = (z_1, \cdots, z_n, z_{n+1}, \cdots, z_{2n})^{\mathrm{T}}, \quad H_{\boldsymbol{z}} = \Big(\dfrac{\partial H}{\partial z_1}, \cdots, \dfrac{\partial H}{\partial z_n}, \dfrac{\partial H}{\partial z_{n+1}}, \cdots, \dfrac{\partial H}{\partial z_{2n}}\Big)^{\mathrm{T}}, \\ \boldsymbol{J} = \begin{pmatrix} \boldsymbol{0} & \boldsymbol{I}_n \\ -\boldsymbol{I}_n & \boldsymbol{0} \end{pmatrix}, \end{cases} \tag{2}$$

in which $\boldsymbol{I}_n$ is the n-dimensional identity matrix, $\boldsymbol{J}$ is called the standard symplectic matrix which has the property $\boldsymbol{J}^{-1} = \boldsymbol{J}^{\mathrm{T}} = -\boldsymbol{J}$, and H is called the Hamiltonian function of the system.

A Hamiltonian system is called the Hamiltonian function. $H(\boldsymbol{z})$ is a quadratic form of $\boldsymbol{z}$,

$$H(\boldsymbol{z}) = \frac{1}{2}\boldsymbol{z}^{\mathrm{T}}\boldsymbol{C}\boldsymbol{z}, \tag{3}$$

where $\boldsymbol{C}$ is a symmetrical matrix $\boldsymbol{C}^{\mathrm{T}} = \boldsymbol{C}$. Thus, the Hamiltonian canonical equation (1) can be expressed as

$$\boldsymbol{J}\dot{\boldsymbol{z}} = \boldsymbol{C}\boldsymbol{z}. \tag{4}$$

The symplectic scheme can be used to solve the linear Hamiltonian equation (4)

$$\boldsymbol{J}\frac{\boldsymbol{z}^{k+1} - \boldsymbol{z}^k}{\tau} = \boldsymbol{C}\frac{\boldsymbol{z}^{k+1} + \boldsymbol{z}^k}{2}, \tag{5}$$

in which τ is the time step. The transformation $\boldsymbol{z}^k \mapsto \boldsymbol{z}^{k+1}$ is given by the following relationship:

$$\boldsymbol{z}^{k+1} = \boldsymbol{F}_\tau \boldsymbol{z}^k, \quad \boldsymbol{F}_\tau = \phi\Big(-\frac{\tau}{2}\boldsymbol{J}^{-1}\boldsymbol{C}\Big), \quad \phi(\lambda) = \frac{1-\lambda}{1+\lambda}. \tag{6}$$

3 Linear Birkhoffian system

The Birkhoffian system is

$$\boldsymbol{K}\frac{\mathrm{d}\boldsymbol{z}}{\mathrm{d}t}-\Big(\frac{\partial B(\boldsymbol{z},t)}{\partial \boldsymbol{z}}+\frac{\partial \boldsymbol{R}(\boldsymbol{z},t)}{\partial t}\Big)=0, \tag{7}$$

where $\boldsymbol{K}$ is an antisymmetric matrix, $B(\boldsymbol{z},t)$ is called the Birkhoffian function, and $\boldsymbol{R}(\boldsymbol{z},t)$ is called the Birkhoffian function group.

When the Birkhoffian function and the Birkhoffian function group satisfy Eq. (8) at the same time,

$$\begin{cases} B=\dfrac{1}{2}\boldsymbol{z}^{\mathrm{T}}\boldsymbol{L}\boldsymbol{z}, \\ \dfrac{\partial B}{\partial \boldsymbol{z}}=\dfrac{1}{2}(\boldsymbol{L}+\boldsymbol{L}^{\mathrm{T}})\boldsymbol{z}, \\ \dfrac{\partial \boldsymbol{R}}{\partial t}=\boldsymbol{S}\boldsymbol{z}. \end{cases} \tag{8}$$

The Birkhoffian system (7) can also be expressed as

$$\boldsymbol{K}\dot{\boldsymbol{z}}=\boldsymbol{P}\boldsymbol{z}, \tag{9}$$

where $\boldsymbol{P}=\frac{1}{2}(\boldsymbol{L}+\boldsymbol{L}^{\mathrm{T}})\boldsymbol{z}+\boldsymbol{S}$, and $\boldsymbol{P}$ is a symmetric matrix which is called the characteristic control of the linear Birkhoffian equation matrix. Equation (8) satisfying Eq. (9) is called a linear Birkhoffian equation. Similarly, the symplectic Euler midpoint scheme can be used to solve the generalized linear Birkhoffian equation (9). The solution form is

$$\boldsymbol{K}\frac{\boldsymbol{z}^{k+1}-\boldsymbol{z}^{k}}{\tau}=\boldsymbol{P}\frac{\boldsymbol{z}^{k+1}+\boldsymbol{z}^{k}}{2}. \tag{10}$$

It can also be expressed as

$$\boldsymbol{z}^{k+1}=\Big(\boldsymbol{K}-\frac{\tau\boldsymbol{P}}{2}\Big)^{-1}\Big(\boldsymbol{K}+\frac{\tau\boldsymbol{P}}{2}\Big)\boldsymbol{z}^{k}. \tag{11}$$

4 Galerkin finite element method for linear Hamiltonian system

4.1 Galerkin finite element method and the weak formulation

In this section, the Galerkin finite element method is used to discretize the linear Hamiltonian equation (4).

Assuming that there are l elements after the system is discretized, the ith element is analyzed below. According to the basic theory of the finite element, its displacement response can be approximately expressed in the form of shape function,

$$\boldsymbol{z}_i=\boldsymbol{N}_i\boldsymbol{z}_i^e, \tag{12}$$

where $\boldsymbol{N}_i=(\boldsymbol{N}_{i1},\boldsymbol{N}_{i2},\cdots,\boldsymbol{N}_{ij})$ is the $(2n\times 2nj)$-dimensional finite element shape function matrix. $\boldsymbol{z}_i^e=(\boldsymbol{z}_{i1}^e,\boldsymbol{z}_{i2}^e,\cdots,\boldsymbol{z}_{ij}^e)^{\mathrm{T}}$ is the $2nj\times 1$ displacement response vector, where j is the number of unit nodes. $\boldsymbol{N}_{im}\,(m=1,2,\cdots,j)$ is the $(2n\times 2n)$-dimensional shape function matrix corresponding to the mth element node. $\boldsymbol{z}_{im}^e=(z_{im1}^e,z_{im2}^e,\cdots,z_{im2n}^e)^{\mathrm{T}}(m=1,2,\cdots,j)$ is the corresponding $(2n\times 1)$-dimensional displacement response vector. e denotes the node value.

Similarly, the velocity response $\dot{\boldsymbol{z}}_i$ of the ith element can also be approximately expressed in the form of a shape function,

$$\dot{\boldsymbol{z}}_i=\boldsymbol{N}_i\dot{\boldsymbol{z}}_i^e, \tag{13}$$

where $\dot{\boldsymbol{z}}_i^e = (\dot{\boldsymbol{z}}_{i1}^e, \dot{\boldsymbol{z}}_{i2}^e, \cdots, \dot{\boldsymbol{z}}_{ij}^e)^{\mathrm{T}}$ is the $(2n \times 1)$-dimensional velocity response vector corresponding to the mth element node.

Obviously, the approximate expressions (12)–(13) of displacement response $\boldsymbol{z}_i$ and velocity response $\dot{\boldsymbol{z}}_i$ cannot accurately meet the linear Hamiltonian equation (4), which will produce residuals,

$$\boldsymbol{R}_i = \boldsymbol{J}\dot{\boldsymbol{z}}_i - \boldsymbol{C}\boldsymbol{z}_i. \tag{14}$$

The approximation method requires that the sum of the weighted residuals in the whole region Ω is 0, that is,

$$\int_\Omega \boldsymbol{W}_m \boldsymbol{R}_i \mathrm{d}\Omega = \int_\Omega \boldsymbol{W}_m (\boldsymbol{J}\dot{\boldsymbol{z}}_i - \boldsymbol{C}\boldsymbol{z}_i)\mathrm{d}\Omega = \boldsymbol{0}, \quad m = 1, 2, \cdots, j, \tag{15}$$

where $\boldsymbol{W}_m\,(m = 1, 2, \cdots, j)$ is the $(2n \times 2n)$-dimensional weighting function matrix of the mth element node.

If we select different weighting functions $\boldsymbol{W}_m\,(m = 1, 2, \cdots, j)$, different approximation methods will be obtained. For the Galerkin finite element method, the weighting function $\boldsymbol{W}_m$ is taken as the shape function $\boldsymbol{N}_{im}$. Thus, the Galerkin finite element equation of linear Hamiltonian system (4) is obtained,

$$\int_\Omega \boldsymbol{N}_{im} (\boldsymbol{J}\dot{\boldsymbol{z}}_i - \boldsymbol{C}\boldsymbol{z}_i)\mathrm{d}\Omega = \boldsymbol{0}, \quad m = 1, 2, \cdots, j. \tag{16}$$

Otherwise, the whole unit is written as

$$\int_\Omega \boldsymbol{N}_i^{\mathrm{T}} (\boldsymbol{J}\dot{\boldsymbol{z}}_i - \boldsymbol{C}\boldsymbol{z}_i)\mathrm{d}\Omega = \boldsymbol{0}. \tag{17}$$

4.2 The symplectic solution

The approximate expressions (12)–(13) of displacement response $\boldsymbol{z}_i$ and velocity response $\dot{\boldsymbol{z}}_i$ are substituted into Eq. (17),

$$\int_\Omega \boldsymbol{N}_i^{\mathrm{T}} \boldsymbol{J} \boldsymbol{N}_i \dot{\boldsymbol{z}}_i^e \mathrm{d}\Omega = \int_\Omega \boldsymbol{N}_i^{\mathrm{T}} \boldsymbol{C} \boldsymbol{N}_i \boldsymbol{z}_i^e \mathrm{d}\Omega. \tag{18}$$

Equation (18) can be further written as

$$\Big(\int_\Omega \boldsymbol{N}_i^{\mathrm{T}} \boldsymbol{J} \boldsymbol{N}_i \mathrm{d}\Omega \Big) \dot{\boldsymbol{z}}_i^e = \Big(\int_\Omega \boldsymbol{N}_i^{\mathrm{T}} \boldsymbol{C} \boldsymbol{N}_i \mathrm{d}\Omega \Big) \boldsymbol{z}_i^e. \tag{19}$$

Let

$$\boldsymbol{A} = \int_\Omega \boldsymbol{N}_i^{\mathrm{T}} \boldsymbol{J} \boldsymbol{N}_i \mathrm{d}\Omega, \quad \boldsymbol{D} = \int_\Omega \boldsymbol{N}_i^{\mathrm{T}} \boldsymbol{C} \boldsymbol{N}_i \mathrm{d}\Omega. \tag{20}$$

Then, the matrices $\boldsymbol{A}$ and $\boldsymbol{D}$ are both $(2nj \times 2nj)$-dimensional square matrices. Thus, Eq. (19) can be further written as

$$\boldsymbol{A}\dot{\boldsymbol{z}}_i^e = \boldsymbol{D}\boldsymbol{z}_i^e. \tag{21}$$

For matrix $\boldsymbol{A}$, since $\boldsymbol{J}$ is an antisymmetric matrix, there is

$$(\boldsymbol{N}_i^{\mathrm{T}} \boldsymbol{J} \boldsymbol{N}_i)^{\mathrm{T}} = \boldsymbol{N}_i^{\mathrm{T}} \boldsymbol{J}^{\mathrm{T}} \boldsymbol{N}_i = -\boldsymbol{N}_i^{\mathrm{T}} \boldsymbol{J} \boldsymbol{N}_i. \tag{22}$$

Thus, $\boldsymbol{N}_i^{\mathrm{T}} \boldsymbol{J} \boldsymbol{N}_i$ is matrix $\boldsymbol{A}$, since $\boldsymbol{J}$ is an antisymmetric matrix.

For matrix $\boldsymbol{D}$, since $\boldsymbol{C}$ is a symmetric matrix, there is

$$(\boldsymbol{N}_i^{\mathrm{T}}\boldsymbol{C}\boldsymbol{N}_i)^{\mathrm{T}} = \boldsymbol{N}_i^{\mathrm{T}}\boldsymbol{C}^{\mathrm{T}}\boldsymbol{N}_i = \boldsymbol{N}_i^{\mathrm{T}}\boldsymbol{C}\boldsymbol{N}_i. \tag{23}$$

Thus, $\boldsymbol{N}_i^{\mathrm{T}}\boldsymbol{C}\boldsymbol{N}_i$ is a symmetric matrix, and $\boldsymbol{D}$ is a symmetric matrix.

Therefore, Eq. (21) is the generalized linear Hamiltonian equation (9).

By assembling the element finite element equation (21), the overall finite element equation of the system can be obtained as

$$\boldsymbol{A}^{\mathrm{all}}\dot{\boldsymbol{z}}_i^{\mathrm{e\_all}} = \boldsymbol{D}^{\mathrm{all}}\boldsymbol{z}_i^{\mathrm{e\_all}}, \tag{24}$$

where matrices $\boldsymbol{A}^{\mathrm{all}}$ and $\boldsymbol{D}^{\mathrm{all}}$ are the overall matrices formed by connecting $\boldsymbol{A}$ and $\boldsymbol{D}$ of all the elements, respectively. Its dimension is $(l+1)nj \times (l+1)nj$. $\boldsymbol{z}_i^{\mathrm{e\_all}}$ and $\dot{\boldsymbol{z}}_i^{\mathrm{e\_all}}$ are, respectively, the displacement response vector and velocity response vector of the overall finite element of the system with dimension n. e_all denotes the overall nodes of the system.

The symplectic preserving Euler midpoint scheme can be used to solve the overall finite element equation (24) of the system. The format is

$$\boldsymbol{A}^{\mathrm{all}}\frac{(\boldsymbol{z}_i^{\mathrm{e\_all}})^{k+1} - (\boldsymbol{z}_i^{\mathrm{e\_all}})^{k}}{\tau} = \boldsymbol{D}^{\mathrm{all}}\frac{(\boldsymbol{z}_i^{\mathrm{e\_all}})^{k+1} + (\boldsymbol{z}_i^{\mathrm{e\_all}})^{k}}{2}. \tag{25}$$

It also can be written as

$$(\boldsymbol{z}_i^{\mathrm{e\_all}})^{k+1} = \Big((\boldsymbol{A}^{\mathrm{all}}) - \frac{\tau\boldsymbol{D}^{\mathrm{all}}}{2}\Big)^{-1}\Big((\boldsymbol{A}^{\mathrm{all}}) + \frac{\tau\boldsymbol{D}^{\mathrm{all}}}{2}\Big)(\boldsymbol{z}_i^{\mathrm{e\_all}})^{k}. \tag{26}$$

After solving Eq. (26), we can get $\boldsymbol{z}_i^{\mathrm{e\_all}}$. The displacement response of the element can be obtained by substituting it into Eq. (12).

So far, the symplectic solution of Galerkin finite element method for the linear Birkhoffian system has been realized.

5 Numerical examples

This section provides two numerical examples to demonstrate the effectiveness of the proposed method (HSFE), i.e., the Bernoulli-Euler cantilever beam vibration and the laminated plate vibration. For comparison, the results obtained by this method are compared with those obtained by the second-order and fourth-order Runge-Kutta algorithms (HSFE, RK_2, and RK_4, respectively).

5.1 Solution of a linear Hamiltonian function

Consider the Hamiltonian function of the 2D linear system,

$$H(p_1, q_1, p_2, q_2) = 1/2(40p_1^2 + 1/20p_2^2 + 160q_1^2 + 1/5q_2^2).$$

The corresponding regular equations are

$$\begin{aligned} &p_1' = -160q_1, \quad p_2' = -1/5q_2, \\ &q_1' = 40p_1, \quad q_2' = 1/20p_2, \\ &p_1(0) = 2, \quad p_2(0) = 2, \quad q_1(0) = 0, \quad q_2(0) = 0. \end{aligned}$$

The analytical solutions to the equation are

$$p_1 = 2\cos(80t), \quad q_1 = \sin(80t), \quad p_2 = 2\cos(t/10), \quad q_2 = \sin(t/10).$$

The results calculated by the HSFE method are as follows.

As shown in Table 1, the time step is set to $\tau = 0.002\,\mathrm{s}$. From Fig. 1, we can see that the phasing orbit of the generalized displacement is a closed ellipse. This shows that the HSFE method can maintain the orbital stability of the linear Hamiltonian system for a long time. As shown in Fig. 2, the analytical solution is almost consistent with the results calculated with the HSFE method, which verifies the accuracy of the proposed method. From Table 1, in $[0, 40\,000\,000]$ steps, the energy error of the calculation results using the HSFE method shows periodic changes.

Table 1 Error between numerical solution and real solution at nodes

Parameter	τ	$10^2\tau$	$10^3\tau$	$10^4\tau$	$10^5\tau$	$10^6\tau$	$10^7\tau$
p_2	10^{-3}	5.645×10^{-7}	5.748×10^{-5}	0.005 7	0.327 4	0.002 5	0.195 1
q_2	2×10^{-3}	2.258×10^{-6}	2.298×10^{-4}	0.022 5	0.118 8	0.009 8	0.357 5

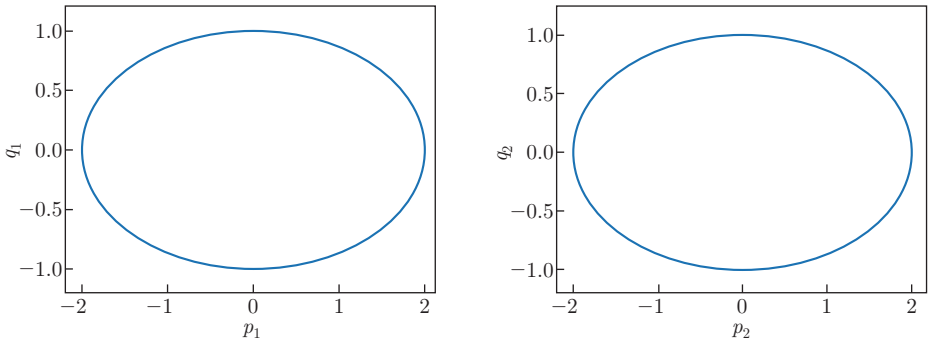

Fig. 1 Phase space curve (color online)

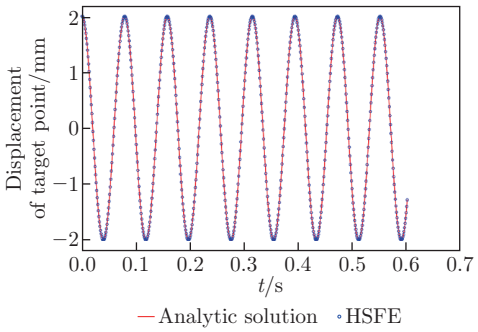

Fig. 2 Displacement-time curve (color online)

5.2 Bernoulli-Euler cantilever beam vibration

As shown in Fig. 3, a rectangular cantilever beam is fixed on the left side, and a downward load is imposed on the beam. The rectangular beam is 9 m long, and its section is illustrated in Fig. 3, in which $a = 0.05\,\mathrm{m}$, and $b = 0.04\,\mathrm{m}$. The thickness of the beam is 0.005 m, and the beam is divided into fifteen elements. The density of the beam is $7.85 \times 10^3\,\mathrm{kg/m^3}$, and Young's modulus is 200 GPa.

The proposed symplectic algorithm is used to obtain the vertical displacement of the right node of element 15, and the Runge-Kutta algorithms are also conducted for comparison. The time step is set to be $\tau = 0.001\,\mathrm{s}$. The results of the vertical displacement and Hamiltonian function are shown in Fig. 4 and Fig. 5, respectively.

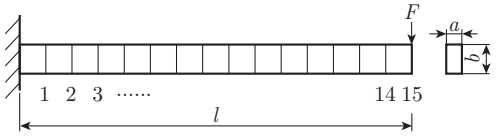

Fig. 3 Finite element model of the cantilever beam

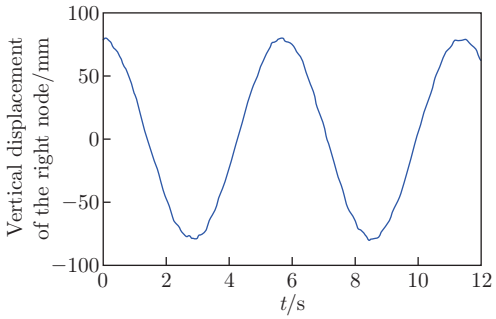

Fig. 4 Deflection responses of the right node of the cantilever beam (color online)

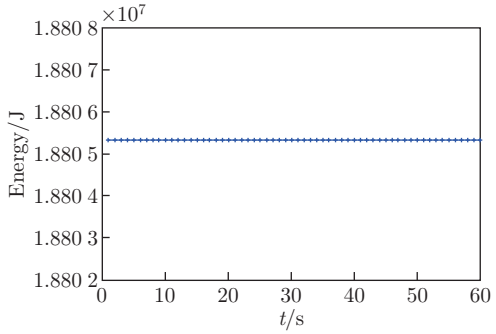

Fig. 5 Overall energy of cantilever beam (color online)

The Butcher tableau for the Runge-Kutta algorithm of order 2 (RK_2) in the study is listed as follows:

$$\begin{array}{c|cc} 0 & & \\ 1 & 1 & \\ \hline & 1/2 & 1/2 \end{array}. \tag{27}$$

The Butcher tableau for the Runge-Kutta algorithm of order 4 (RK_4) in the study is listed as follows:

$$\begin{array}{c|cccc} 0 & & & & \\ 1/2 & 1/2 & & & \\ 1/2 & 0 & 1/2 & & \\ 1 & 0 & 0 & 1 & \\ \hline & 1/6 & 1/3 & 1/3 & 1/6 \end{array}. \tag{28}$$

From the results, we can conclude that the proposed algorithm can obtain reasonable results of the vertical displacement[31].

As shown in Fig. 4, in the first 12 s, the vibration response of the right end node presents the shape of the sinusoidal curve, which conforms to the physical law of node responses. The Hamiltonian function remains a constant value during the numerical calculation as shown in Fig. 5, which illustrates the symplectic conservation of the proposed algorithm. The symplectic properties of the algorithm can be carried out by the values of the Hamiltonian function with respect to time.

As shown in Fig. 6, HSFE, RK_2, and RK_4 are used to calculate the responses of the right nodes within the first 0.012 s. Through comparison, it can be found that the stability of HSFE is stronger than the other traditional algorithms, the vibration response of nodes calculated with RK_2 has diverged, and the calculation methods of RK_4 and HSFE are still relatively stable. In Fig. 7, compared with the RK_4, in the first 60 s, HSFE method can keep the energy stable, while the energy of the RK_4 method shows a downward trend, and thus it can be explained that HSFE method is more stable.

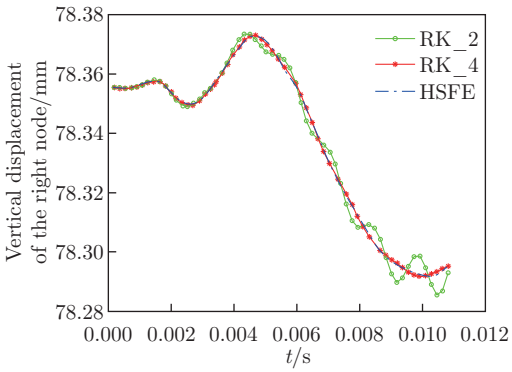

Fig. 6 Short-term deflection response of the right node of the cantilever beam based on different algorithms (color online)

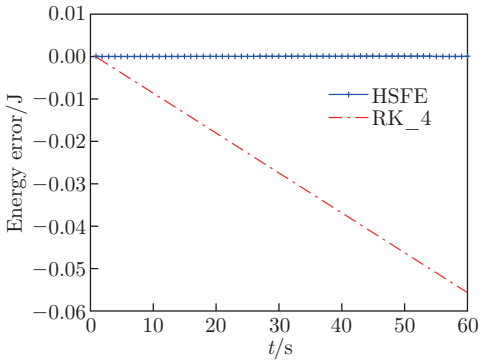

Fig. 7 Long-term Hamiltonian function of the right node of the cantilever beam based on different algorithms (color online)

5.3 Laminated plate vibration

The last example concerns a fully clamped composite laminate with the side length $a = 1.6\,\mathrm{m}$, the width $b = 0.8\,\mathrm{m}$, and the mass density $\rho = 1\,500\,\mathrm{kg/m^3}$ as shown in Fig. 8, while the thickness of each layer $h = 0.1\,\mathrm{mm}$.

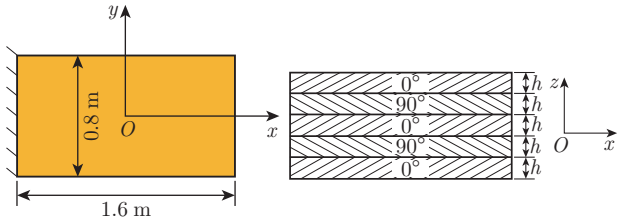

Fig. 8 Laminated plate with one end under clamping (color online)

The dispersion in the material properties introduced by the material production and measurement process is unavoidable. The nominal and perturbed parts of the material properties are $E_1 = 38.6\,\mathrm{GPa}$, $E_{1\mathrm{r}} = 5\% \times E_1$, $E_2 = 8.27\,\mathrm{GPa}$, $E_{2\mathrm{r}} = 5\% \times E_2$, $\nu_{21} = 0.26$, $\nu_{21\mathrm{r}} = 10\% \times \nu_{21}$, $G_{12} = 4.14\,\mathrm{GPa}$, and $G_{12\mathrm{r}} = 7\% \times G_{12}$.

The response caused by the force $F = -1\,000\,\mathrm{N}$ acts on the center of the laminate in order. The HSFE method proposed in this paper and the traditional Runge-Kutta algorithm are used to solve the dynamic response of the midpoint at the right end of the cantilever plate structure, and the comparative analysis is carried out at the two levels of energy and stability of the calculation results.

As shown in Fig. 9, the response of the laminate in the first $2.5 \times 10^{-6}\,\mathrm{s}$ conforms to the trend of the continuous solution, which is similar to the traditional solution[32]. Figure 10 shows that the Hamiltonian function of the right node can keep constant values in 1 s. However, it is worth noting that the numerical results calculated with the RK_2 are exponentially divergent under the condition of the set time step in a short time interval $t \in [0, 2 \times 10^{-7}]\,\mathrm{s}$ as shown in Fig. 11, while there is not any difference between the amplitude calculated by the Runge-Kutta method and the HESM method. Only when the time step is extremely small like $\tau = 10^{-8}\,\mathrm{s}$, satisfactory results can be achieved. As shown in Fig. 12, the system energy value calculated

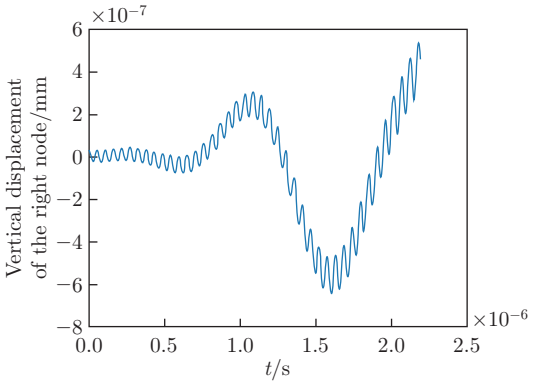

Fig. 9 Deflection responses of the right node of the laminated plate (color online)

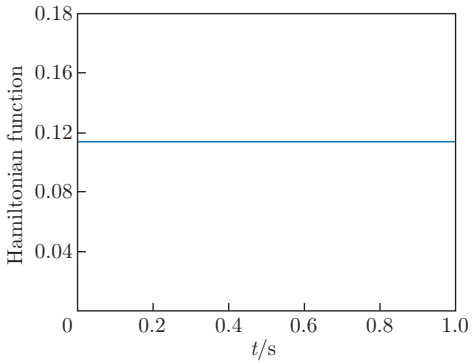

Fig. 10 Energy change of the laminated plate in the first second (color online)

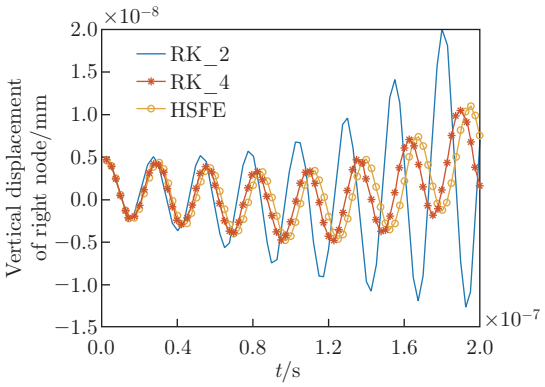

Fig. 11 Short-term deflection response of the right joint of the composite plate based on different algorithms (color online)

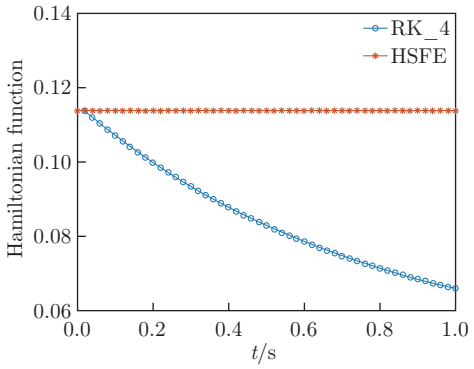

Fig. 12 Long-term Hamiltonian function of the right node of the laminated plate based on different algorithms (color online)

with the RK_4 method shows a downward trend, because the method itself is a dissipation algorithm, and numerical damping will occur in the calculation process. On the contrary, the HSFE method shows an outstanding advantage in terms of stability. This phenomenon highlights the superiority of HSFE.

6 Conclusions

This paper presents a finite element method for solving the dynamic problems of linear continuum. It is used to solve the vibration problems of linear continuous systems, avoiding energy loss in the solving process. First, we discretize the continuum into finite elements. Then, the generalized displacement vector is defined. The Hamiltonian structure of the element is constructed, the continuous system is discretized with the finite element method based on Galerkin, and then the velocity and displacement responses of the continuum are interpolated to obtain the linear Birkhoffian system. After that, it is solved by the Euler midpoint scheme. By using the proposed method, a series of vibration response problems of linear elastic bodies can be solved, and finally, the solution without energy dissipation can be obtained.

The validity, symplectic conservation, and engineering applicability of HSFE are studied by two examples. Compared with the Runge-Kutta method, the HSFE method can obtain high-precision results in a longer term, especially in the case that the Runge-Kutta method cannot converge. Only when the Runge-Kutta method takes a very short time step and takes the fourth-order accuracy, it can obtain high accuracy results. Therefore, the HSFE method can effectively improve computational efficiency. In addition, in terms of energy, the HSFE method can keep the conservation for long-term dynamics, while the energy of the traditional Runge-Kutta algorithm gradually decreases with the increase in time.

Conflict of interest The authors declare no conflict of interest.

Acknowledgements The authors wish to express their many thanks to the reviewers for their useful and constructive comments.

References

[1] GONZALEZ, O. Exact energy and momentum conserving algorithms for general models in nonlinear elasticity. *Computer Methods in Applied Mechanics and Engineering*, **190**(13-14), 1763–1783 (2000)

[2] GONZALEZ, O. Time integration and discrete Hamiltonian systems. *Journal of Nonlinear Science*, **6**(5), 449–467 (1996)

[3] GONZALEZ, O. and SIMO, J. C. On the stability of symplectic and energy-momentum algorithms for non-linear Hamiltonian systems with symmetry. *Computer Methods in Applied Mechanics and Engineering*, **134**(3-4), 197–222 (1996)

[4] KRENK, S. Energy conservation in Newmark based time integration algorithms. *Computer Methods in Applied Mechanics and Engineering*, **195**(44-47), 6110–6124 (2006)

[5] SIMO, J. C. and TARNOW, N. The discrete energy-momentum method-conserving algorithms for nonlinear elastodynamics. *Zeitschrift für Angewandte Mathematik und Physik*, **43**(5), 757–792 (1992)

[6] SIMO, J. C., TARNOW, N., and DOBLARE, M. Non-linear dynamics of three-dimensional rods: exact energy and momentum conserving algorithms. *International Journal for Numerical Methods in Engineering*, **38**(9), 1431–1473 (2010)

[7] SIMO, J. C., TARNOW, N., and WONG, K. K. Exact energy-momentum conserving algorithms and symplectic schemes for nonlinear dynamics. *Computer Methods in Applied Mechanics and Engineering*, **100**(1), 63–116 (1992)

[8] FENG, K. On difference schemes and symplectic geometry. *Proceedings of the* 1984 *Beijing Symposium on Differential Geometry and Differential Equations*, Science Press, Beijing, 42–58 (1985)

[9] KANG, F., WU, H., and QIN, M. Symplectic difference schemes for linear Hamiltonian canonical systems. *Journal of Computational Mathematics*, **8**(4), 371–380 (1990)

[10] KHANG, A., HOWSMON, D. P., LEJEUNE, E., and SACKS, M. S. *Multi-scale Modeling of the Heart Valve Interstitial Cell*, *Multi-Scale Extracellular Matrix Mechanics and Mechanobiology*, Springer International Publishing AG, Cham, 21–53 (2020)

[11] SANZ-SERNA, J. M. Runge-Kutta schemes for Hamiltonian systems. *BIT Numerical Mathematics*, **28**(4), 877–883 (1988)

[12] LASAGNI, F. M. Canonical Runge-Kutta methods. *Zeitschrift für Angewandte Mathematik und Physik*, **39**(6), 952–953 (1988)

[13] SURIS, Y. B. On the conservation of the symplectic structure in the numerical solution of Hamiltonian systems. *Numerical Solution of Ordinary Differential Equations*, **232**, 148–160 (1988)

[14] BRIDGES, and THOMAS, J. Multi-symplectic structures and wave propagation. *Mathematical Proceedings of the Cambridge Philosophical Society*, **121**(1), 147–190 (1997)

[15] REICH, S. Multi-symplectic Runge-Kutta collocation methods for Hamiltonian wave equations. *Journal of Computational Physics*, **157**(2), 473–499 (2000)

[16] YAN, X., VEGT, J., and BOKHOVE, O. Discontinuous Hamiltonian finite element method for linear hyperbolic systems. *Journal of Scientific Computing*, **35**, 241–265 (2008)

[17] XU, Y., VAN DER VEGT, J. J. W., and BOKHOVE, O. Discontinuous Hamiltonian finite element method for linear hyperbolic systems. *Journal of Scientific Computing*, **35**(2-3), 241–265 (2008)

[18] KIRBY, R. C. and KIEU, T. T. Symplectic-mixed finite element approximation of linear acoustic wave equations. *Numerische Mathematik*, **130**(2), 257–291 (2015)

[19] SÁNCHEZ, M., CIUCA, C., NGUYEN, N. C., PERAIRE, J., and COCKBURN, B. Symplectic Hamiltonian HDG methods for wave propagation phenomena. *Journal of Computational Physics*, **350**, 951–973 (2017)

[20] APPELO, D. and HAGSTROM, T. An energy-based discontinuous Galerkin discretization of the elastic wave equation in second order form. *Computer Methods in Applied Mechanics & Engineering*, **338**, 362–391 (2018)

[21] QIU, Z. P. and JIANG, N. A symplectic conservative perturbation series expansion method for linear Hamiltonian systems with perturbations and its applications. *Advances in Applied Mathematics and Mechanics*, **13**(6), 1535–1557 (2021)

[22] QIU, Z. and XIA, H. Symplectic perturbation series methodology for non-conservative linear Hamiltonian system with damping. *Acta Mechanica Sinica*, **37**, 983–996 (2021)

[23] QIU, Z. P. and JIANG, N. Comparative study and application of random and interval inhomogeneous linear Hamiltonian systems (in Chinese). *Chinese Journal of Theoretical and Applied Mechanics*, **52**, 60–72 (2020)

[24] QIU, Z. P. and JIANG, N. Random and interval uncertainty symplectic preserving algorithms for linear Birkhoff equations and their comparative studies (in Chinese). *Chinese Science*: *Physics*, *Mechanics*, *Astronomy*, **50**(8), 084611 (2020)

[25] ZHOU, S., MA, Y. C., SUN, Z., and HU, X. F. A novel super symplectic analytical singular element for crack propagation along a bimaterial interface. *Theoretical and Applied Fracture Mechanics*, **122**, 103565 (2022)

[26] SU, B., SHEN, W., LANG, C., and LI, H. Order-corrected symplectic finite element method for elastic wave modelling. *Exploration Geophysics*, **52**, 321–334 (2020)

[27] SUN, Z., HU, G., NIE, X., and SUN, J. An analytical symplectic method for buckling of ring-stiffened graphene platelet-reinforced composite cylindrical shells subjected to hydrostatic pressure. *Journal of Marine Science & Engineering*, **10**(12), 1834 (2022)

[28] LAI, A., FU, G., and LIU, P. A symplectic analytical approach for torsional buckling of cylindrical shells with asymmetric local defects. *International Journal of Structural Stability and Dynamics*, **23**, 2350093 (2022)

[29] CHEN, G. and ZHU, G. Symplectic algorithms for stable manifolds in control theory. *IEEE Transactions on Automatic Control*, **67**(6), 3105–3111 (2022)

[30] ZHOU, Z., FAN, J., LIM, C. W., RONG, D., and XU, X. A size-dependent coupled symplectic and finite element method for steady-state forced vibration of built-up nanobeam systems. *International Journal of Structural Stability & Dynamics*, **19**(7), 1950081 (2019)

[31] SHIRAZI, H. M. S. and KOUROSH, H. A new approach to analytical solution of cantilever beam vibration with nonlinear boundary condition. *Journal of Computational and Nonlinear Dynamics*, **7**(3), 034502 (2012)

[32] SHEN, Y. and GIBBS, B. M. An approximate solution for the bending vibrations of a combination of rectangular thin plates. *Journal of Sound and Vibration*, **105**(1), 73–90 (1986)